J-Researchers

JOURNAL OF CIVIL ENGINEERING RESEARCHERS

Evaluation of Mechanical Properties and Microstructure of Pozzolanic Geopolymer Concrete Reinforced with Polymer Fiber

Mohammadhossein Mansourghanaei[a*]

[a] *Ph.D. in Civil Engineering, Department of Civil Engineering, Chalous Branch, Islamic Azad University, Chalous, Iran*

Journals-Researchers use only: Received date: 2023.04.10; revised date: date 2023.05.21; accepted date: 2023.05.27

Abstract

in recent decades, Geopolymer concrete (GPC) is a new material in the construction industry, which has favorable performance and workability and contains aluminosilicate materials full of silicate (Si), aluminum (Al), and alkaline solution as a binder. The advantages of using geopolymer materials instead of cement in concrete are not limited to high mechanical and microstructural properties. It also has a remarkable effect in reducing greenhouse gas emissions. In the current study, Granulated Blast Furnace Slag (GBFS) GPC was used with 0-2% polyolefin fibers (POFs) and 0-8% nano-silica (NS) to improve its structure. After curing the specimens under dry conditions at a temperature of 60 °C in an oven, they were subjected to compressive strength, tensile strength, elastic modulus, ultrasonic pulse velocity (UPV) and impact resistance tests to evaluate their mechanical properties. The addition of NS enhanced the whole properties of the GBFS geopolymer concrete. The compressive strength, tensile strength, and elastic modulus of the concrete increased by up to 22%, 14%, and 24%, respectively. Besides, it leads to ultrasonic wave velocity enhancement to 12% in the room temperature. The addition of the fibers to the GPC significantly increased the tensile strength (by up to 9%) and the energy absorbed due to the impact. Moreover, compared to Concrete containing ordinary portland cement (OPC), the GPC demonstrated much better mechanical and microstructural properties. Besides, the presence of POFs in the GPC compound substantially affects tensile strength and resistance against an impact. Accordingly, the sample's tensile strength had an improvement by 8.4% in the room temperature. In the following, by conducting the X-Ray Fluorescence (XRF), X-Ray Diffraction (XRD), and Scanning electron microscope (SEM) tests, a microstructure investigation was carried out on the concrete samples. In addition to their overlapping with each other, the results indicate the GPC superiority over the regular concrete. (DOI:**https//doi.org/10.52547/JCER.5.1.1**)

Keywords :
Geopolymer Concrete, Granulated Blast Furnace Slag, Nanosilica, Polyolefin Fibers, Mechanical Properties, Microstructure.

[*] Corresponding Author. Tel: +989121712070; E-mail: Mhm.Ghanaei@iauc.ac.ir

1. Introduction

GBFS and NS containing abundant aluminosilicate materials are known as synthetic pozzolans. Using this material instead of cement can improve concrete resistance and decrease the increasing demand for its usage in concrete [1,2]. Comparing the concrete containing regular Portland cement with GPC, McNulty [3] asserted that the geopolymer concretes have higher compressive strength. The properties and the bonding type are different in regular and geopolymer concretes. The bonding in regular concretes is based on calcium oxide hydration and silicon dioxide reactions in order to form calcium silicate hydrate. However, the GPC bonding is established via alkaline activator contact with the Aluminosilicate raw materials, reshaped in the polymerization reaction product, and slowly cooled in a high pH medium and hydrothermal condition (hydrothermal condition is referred to the chemical reactions in the presence of solvent in higher pressure and temperature). This structure (related to the geopolymer concrete) has some merits compared to the regular concrete, e.g., it provides better resistance performance at higher temperatures [4]. The presence of NS in GPC not only has a positive effect on its physical and mechanical properties but also accelerates the geopolymer reaction, reduces the system's alkalinity, and thus, lowers the degradation of the used fibers [5]. It also increases the compressive strength of the geopolymer concrete. This rise occurs at the Si/Al ratios of up to 2% in the mixture. However, the addition of more than the optimal value of NS particles, reduces the compressive strength [6]. Improved compressive strength [7], elastic modulus, and UPV have been reported with the use of NS in GPC [8]. Another study on the GPC cured at the ambient temperature has investigated the effect of adding 0% to 10% NS to specimens with different concentrations of activator liquid (NaOH) (M 8, 10, 12). The optimum compressive strength and tensile strength coefficient were obtained by adding 6% NS [7]. Preventing the connection of pores and bonding the flow channels in the concrete, the POFs strengthen it and avoid its spalling [9]. A study on the effect of POFs with various lengths and diameters on different geopolymer concretes has shown that the proper use of fibers raises the tensile strength, elastic modulus, and impact energy. The addition of fibers reduces the compressive strength [10]. The addition of POFs to a concrete beam remarkably improves its strength after cracking by increasing its elastic modulus [11]. The Crack Mouth Opening Displacement (CMOD) analysis has also indicated that the POFs have proper bonding properties and, due to their proper stiffness, they can keep the concrete pieces beside each other after the initial cracking [12]. In a study into the effect of adding 0.5% POFs on the geopolymer concrete, a reduction by 12% to 15% was observed in the compressive strength. The reduction was larger in the specimens containing fibers with a length of 55 mm compared to those with a length of 44 mm [13, 14]. This study mainly aims to investigate the mechanical and microstructural properties of the geopolymer concretes based on the GBFS containing NS and also reinforced with POFs. For this purpose, the compressive and tensile strength, modulus of elasticity, and impact tests have been conducted. In order to accurately analyze the ultrasonic wave's velocity test and also the relationship between the compressive strength and tensile strength, the compressive strength and modulus of elasticity, the compressive strength and ultrasonic wave velocity have also been examined. Ultimately, the microstructure was examined by caused by samples' by SEM, XRF and XRD tests.

2. Experimental Program and Test Methods

2.1 Materials

In this experimental study, the Portland cement type II with a 2.35 gr/cm^3 of specific weight according to standard En 197-1 and the GBFS was used in powder form with the specific weight of 2.45 g/cm^3 according to ASTM C989/C989M standard. The chemical properties of these materials are indicated in Table 1. The used fine aggregates were natural clean sand with a fineness modulus of 2.95 and a specific weight of 2.75 g/cm^3, and the coarse aggregates were crushed gravel with a maximum size of 19 mm and a specific weight of 2.65 g/cm^3 according to the requirements of the ASTM-C33. The curing was performed at a temperature of 60 °C according to the standards of the geopolymer concrete. The NS particles made up of 99.5% SiO_2 with an average diameter in the range of 15 to 25 nm were used. Crimped POFs, 30 mm in length, were also used according to ASTM D7508/D7508M standard. whose physical properties are shown in Tabel. 2.

2.2 Mix Design

Six mix designs according to ACI 211.1-89 standard. one as ordinary concrete (OPCNS0PO0) and five with different NS and polyolefin fiber percentages, were considered in the study. The GPC specimens were divided into two major groups. The first group had no POFs and 0-8% NS. The second group contained 8% NS (GPCNS0PO0, GPCNS4PO0 and GPCNS8PO0) and 1% or 2% POFs (GPNS8PO1 and GPCNS8PO2). A superplasticizer was used to achieve the same workability in all mix designs with a slump of 100±20 mm. Moreover, 202.5 kg/m^3 Alkia alkaline solution was added to the geopolymer specimens. The used alkaline solution is a combination of NaOH and Na_2SiO_3 with the weight ratio of 2.5, utilized with the mixture specific weight of 1483 kg/m^3 and the concentration of 12 M. The conducted studies indicate that due to the significant level of C-S-H formation when utilizing Na_2SiO_3, using a combination of NaOH and Na_2SiO_3 increases the compressive strength compared to single employment of CaOH [15]. Table 3 lists the mix designs of the specimens.

Table1
Chemical Compositions of Materials

Component	GBFS (%)	Portland cement (%)
SiO_2 (%)	29.2	21.3
Al_2O_3 (%)	19.4	4.7
Fe_2O_3 (%)	5.8	4.3
CaO (%)	38.6	62.7
MgO (%)	2.8	2.1
SO_3 (%)	2.6	2
K_2O (%)	0.1	0.65
Na_2O (%)	0.2	0.18
TiO_2 (%)	0.6	-
Free Cao (%)	-	1.12
LOI (%)	0.3	1.84
Blaine (cm^2/g)	2200	3200

Table 2
Physical Properties of The Fiber Steel (FS)

Tensile Strength (N/mm^2)
Length (mm)
Diameter (mm)
Elasticity Modulus (G.Pa)
Bulk Density (g/cm^3)

Table 3
Details of The Mix Designs

Mix ID	Cement	GBFS	Water	Alkaline Solution	NS	Coarse Aggregates	Fine Aggregates	Polyolefin Fibers	Super Plasticizer
	(Kg/m^3)								
OPCNS0PO0	450	0	202.5	0	0	1000	761	0	9
GPCNS0PO0	0	450	0	202.5	0	1000	816	0	9
GPCNS4PO0	0	432	0	202.5	18	1000	767	0	10
GPCNS8PO0	0	414	0	202.5	36	1000	718	0	11
GPCNS8PO1	0	432	0	202.5	36	1000	672	24	11
GPCNS8PO2	0	432	0	202.5	36	1000	646	48	11

2.3 Test Methods

After fabricating the samples, for better curing and increasing the resistance properties, the samples were placed in an oven at 60 °C with a thermal rate of 4.4 °C/min for 48 h. In this study, the compressive strength tests were performed on 100-mm^3 cubic specimens based on BS EN 12390 [16]. Furthermore, to determine the tensile strength of the cylindrical specimens (15 cm in diameter and 30 cm in length), the splitting tests were conducted based on ASTM C496 [17]. The test of modulus of elasticity of concrete under the standard ASTM C469 [18] was carried out on concrete samples (15 cm in diameter and 30 cm in length). The UPV tests [19] were conducted according to ASTM C597 using a non-destructive ultrasonic electronic apparatus, PUNDIT MODEL PC1012, with an accuracy of ±0.1 μs for a transformator with a vibrational frequency of 55 kHz and a movement time accuracy of ±2% for the

distance. The concrete's resistance to dynamic loads (impacts) was measured using the drop weight hammer test according to the report by the ACI 544-2R committee [20]. This test was conducted with repeating impacts on disks with a diameter of 15 cm and a height of 63.5 cm. It should be noted that 264 concrete samples were made in this research. So that for compressive strength (54 samples), tensile strength (54 samples), modulus of elasticity (54 samples), UPV (54 samples) and impact test (36 samples) the results of each stage, the average obtained from performing the test on three laboratory samples Is. In the SEM (6 samples) and XRD (6 samples) tests, the results are based on one sample.

3. Results and Discussion

3.1 Results of The Compressive Strength, Tensile Strength and Elastic Modulus Tests

As shown in Fig. 1 and Fig. 2, with the rise in the POFs content, the compressive strength reduced by 20-22%. The reason for the reduction in the compressive strength of specimens containing POFs can be the micro internal defects in the geopolymer matrix caused by the additional fibers [21], and by adding 1% and 2% fibers, the tensile strength grew by 4% and 8%, respectively. Moreover, the addition of 4% and 8% NS increased the compressive strength by 10% and 22%, and the tensile strength by 11% and 15%, respectively. The standard deviation in the compressive strength test at the ages curing of 7, 28 and 90 days was obtained as 9.08, 8.22 and 7.74, respectively. and the standard deviation in the tensile strength test at the ages curing of 7, 28 and 90 days was obtained as 0.46, 0.48 and 0.37, respectively. The smallness of the standard deviation shows that the data are close to the average and the data has less dispersion. The influence of the NS in improving the strength can be attributed to the following multi-stage mechanism that improves the concrete's microstructures and thus, increases the mechanical properties.

1. The rise in the pozzolanic reaction [5]. The presence of NS in the GPC accelerates the pozzolanic reaction.
2. The filling effect of NS particles [22, 23]. First, the distribution of NS particles besides the other concrete particles results in a denser matrix. Second, the NS's reaction in the geopolymerization procedure produces a larger amount of aluminosilicate gel, along with the reaction products of the main materials. The reaction by-product is likely to deposit in the structure of the existing pores. The rise in SiO_2 increases the matrix density [24]. Therefore, the filling effect of NS is improved by the particle packing, and the by-product produces a denser matrix, reducing the porosity and increasing the strength.
3. It acts as a nucleus [25, 26]. In the C-S-H gel structure, nanoparticles can act as a nucleus and form strong bonds with the C-S particles of the gel. Thus, during the hydration, the products' stability increases, and the durability and mechanical products are expected to improve.

The elastic moduli of specimens are plotted in Fig. 3. The rise in the elastic modulus caused by the addition of 1% and 2% fibers to the specimens was 1.5% and 7%, respectively. Moreover, adding 4% and 8% NS increased the elastic modulus by 12% and 13%, respectively, compared to the specimens without NS. The addition of NS to the fiber-reinforced concrete has two results. First, the concrete density increases, leading to a rise in the elastic modulus. Second, as long as the pores of the concrete are not filled, increasing the NS raises the elastic modulus. However, the excessive increase in the amount of NS results in a lower dynamic elastic modulus.

The standard deviation in the elastic moduli test at the ages curing of 7, 28 and 90 days was obtained as 3.46, 4.32 and 3.73, respectively.

According to the drawing of the standard deviation for the ages curing of 7, 28. 90 days in each three chart, it can be seen that the results in OPC compared to GPC have a big difference with the standard deviation. This is due to the superior mechanical properties of GPC compared to OPC. With the increase of curing age in the samples, the standard deviation values have decreased and this is due to the completion of the hydration process (in OPC) and geopolymerization (in GPC) in concrete.

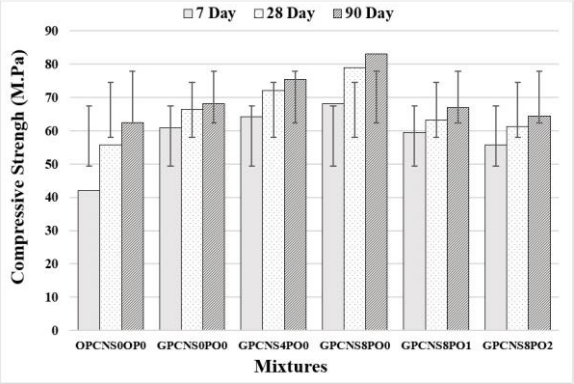

Fig. 1. The Compressive Strengths of The Specimens

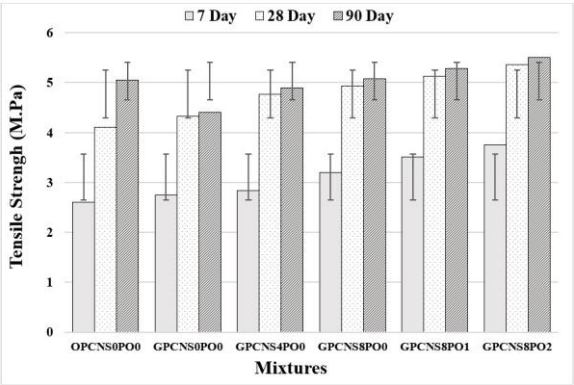

Fig. 2. The Tensile Strengths of The Specimens

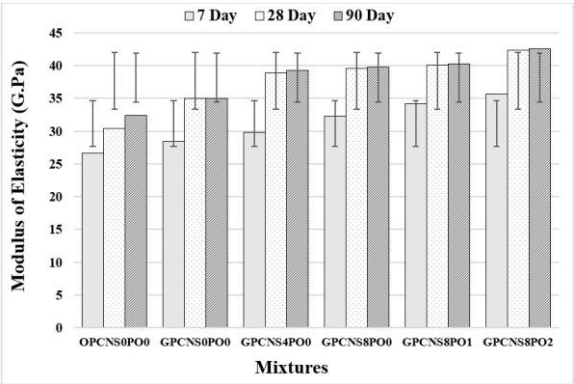

Fig. 3. Elastic Modulus Variations of The Specimens

3.2 Relationship Between The Compressive Strength With Tensile Strength and Elastic Modulus

Table 4 lists the relationships between the compressive and tensile strength (splitting) proposed by various researchers. These relationships are obtained based on the output of the excel chart of compressive strength and tensile strength. In this table Eq. 1 is obtained for ordinary concrete, while Eq. 2 is provided for GPC cured at a temperature of 60 °C in an oven. Eq. 3 is the relationship between the strengths in the GPC cured at the ambient temperature. Eq. 4 is the equation on GPC and OPC obtained in the current study. According to the software information, the difference between relation 1 and relation 4 is 12%, also the error rate in relation 2 is about 8%, the amount of this difference compared to relation 3 is 37%.

Table 5 demonstrates the elastic modulus variations against the changes in the compressive strength. These relationships are obtained based on the output of the excel chart of compressive strength and elastic modulus. The elastic modulus increases with the compressive strength. The predictions of the elastic moduli of the specimens are presented with respect to the compressive strength obtained in the current study using the relationships provided in Table 5. In this table Eq. 5 is for the OPC, and Eqs. 6 and 7 are for the GPC. Eq. 8 is the equation on GPC and OPC obtained in the current study. Relationship number 5 is in good agreement with the relationship obtained from OPC and GPC in this research. The average error value in relation 5, 6 and 7 compared to the laboratory results in this research is about 7, 6 and 28%, respectively, and the large difference of this value in relation 7 is due to the importance of curing at ambient temperature and 60 ℃ for concrete. It is in relationships 7 and 8.

Table 4
Relationships Predicting the Tensile Strength Based on The Compressive Strength

Eq. Number	Equation	Reference
1	$f_t = 0.59\sqrt{f_c}$	ACI363R-92 [27]
2	$f_t = 0.93(f_c)^{0.5}$	Nath [28]
3	$f_t = 0.69(f_c)^{0.5}$	Diaz [29]
4	$f_t = 0.2172(f_c)^{0.7158}$	Present Eq

Table 5
Relationship Between the Elastic Modulus and Compressive Strength of Specimens

Eq. Number	Equation	Reference
5	$E_c = 3320\left(f'_c\right)^{0.5} + 6900$	ACI 363 [30]
6	$E_c = 0.037 \times \rho^{1.5}\left(f_c\right)^{0.5}$	Diaz-Loya et al (GPC) [31]
7	$E_c = 3510\left(f_c\right)^{0.5}$	Pradip and Sarker (GPC) [28]
8	$E_c = 2.3923\left(f_c\right)^{0.6397}$	Present Eq

3.3 The Results of The Ultrasonic Pulse Velocity (UPV) Test

The velocities of the ultrasonic pulses passing through the specimens are shown in Fig. 4. The speed quality of ultrasonic waves based on IS 13311-1 [32] standard in four levels as follows: Doubtful with a speed below 3000 m/s, Moderate with a speed of 3000 to 3500 m/s, Good with a speed of 3500 to 4500 m/s and Excellent with a speed of More than 4500 m/s is divided. UPV method is used to estimate the concrete quality using the regression analysis between the compressive strength and the UPV[19]. The results indicated that the addition of fibers reduced the ultrasonic pulse velocity. This reduction was not significant being in the range lower than 12.5%. The small effect of fibers on the pulse velocity was also reported by Sahmaran et al. They attributed the negligible changes in the pulse velocity to the uniformity of the concrete matrix in all mixtures [33]. According to the obtained results, the whole 28-day and 90-day mix designs were considered in the "Excellent" range [34]. As long as the UPV values are classified as "Excellent", the concrete has no large cracks or pores that can affect the integrity of the specimen structure [35]. On the other hand, the obtained results revealed that the addition of NS increased the pulse velocity by filling the pores and densifying and integrating the concrete. Due to the curing in the dry environment of the oven, some fine cracks and pores were formed in the GPC preventing its full integrity, which allows for the transmission of ultrasonic pulses with higher velocities. Therefore, the obtained velocities were slightly lower than those of ordinary concrete. Nevertheless, these cracks had very fine dimensions and could only influence the UPV having no remarkable effect on the compressive strength of the specimens [36]. lack of fibers and presence of more NS in mix design 4 (GPCNS8PO0) was very effective in making the velocity of the passing pulses close to those of the ordinary concrete. The amount of standard deviation in this test at the curing ages of 7, 28 and 90 days was obtained as 302, 306 and 426, respectively. The higher difference of the results in OPC compared to the standard deviation is due to the lower results in GPC in line with the heat curing in this type of concrete, which has led to the occurrence of micro cracks and the drop in results.

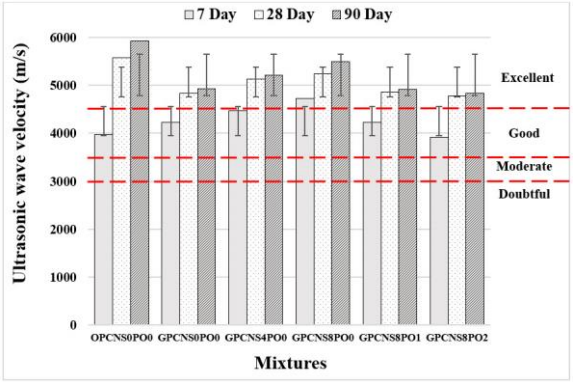

Fig. 4. The Variations in The Ultrasonic Pulse Velocities of The Specimens

3.4. Results of The Impact Resistance Tests

Table 6 shows the results of the impact resistance test. According to Eq. 9, the impact energy (E_n, E_1 for initial cracking and E_2 for final fracture the sample) and the energy absorbed (E_2-E_1) in 90 days by different specimens are shown in Figs. 5 and 6, respectively. In all groups, with the rise in the polyolefin fiber percentage to 1% and 2%, the number of impacts required for both initial crack (N_1) and the final fracture (N_2) increased, i.e., the energy absorption capacity increased with the addition of fibers to the geopolymer concrete. The POFs

effectively resisted the crack initiation and propagation during the fracture of the concrete structure. They also relieved the stress concentration in the tips of the cracks and delayed their damage process under impact loads. With the rise in the loading, the cracks developed near the fibers until the separation could be observed in the surface of fibers in the matrix. Due to the tensile stress formed in the predicted path of cracks, when they reached the surface of fibers, the stress concentration in their tips was reduced, and their path deviated. These conditions prevented further crack propagation. This effect describes the bridging or capacity in limiting the cracks in the fiber-reinforced concrete. The results indicated a much greater effect of POFs on the impact resistance compared to the NS. In the current study, with the addition of 1% and 2% fibers to the specimens, the impact energy caused by the formation of the first crack (E_1) increased by 13% and 30%, respectively. Moreover, the impact energy against full failure (E_2) grew by 213% and 345%, respectively. As the results showed, the addition of fibers was more effective in the full failure compared to the first crack. By considering a ratio E_2/E_1 as flexibility index of concrete, this in fact indicates the imposition of more blows for failure after the initial crack. Therefore, the addition of 1% and 2% fibers increased the flexibility index (E_2/E_1) 2.8 and 3.4 times, respectively. With the addition of 1% and 2% fibers, the amount of absorbed energy (E_2-E_1) became 6.2 and 9.3 times larger, indicating the good ability of fibers in absorbing the impact energy. Adding 4% and 8% NS increased the energy required for the formation of the first crack (E_1) by 62% and 77%, and the energy needed for full failure (E_2) by 46% and 58%, respectively. Compared to the ordinary concrete, the GPC required 44% and 14% higher energy for the first crack (E_1) and the full failure (E_2), respectively.

In figure 5, the amount of standard deviation for E_1, E_2 and E_2/E_1 is 161, 1252 and 1122 respectively. and in Figure 6, the amount of standard deviation for E_2-E_1 is equal to 1122. The large number of standard deviation is due to the dispersion of the results, as it can be seen that the results in GPC containing POFs are much more than other concretes. In this regard GPC containing 2% POFs has the highest dispersion of results.

$$E_n = N \times W \times H \quad \text{(Eq. 9)}$$

E_n: Impact Energy
N: Number of Impacts
W: hammer weight (According to ACI 544.2R = 4.54 kg)
H: Weight throw height (According to ACI 544.2R = 45.7 cm)

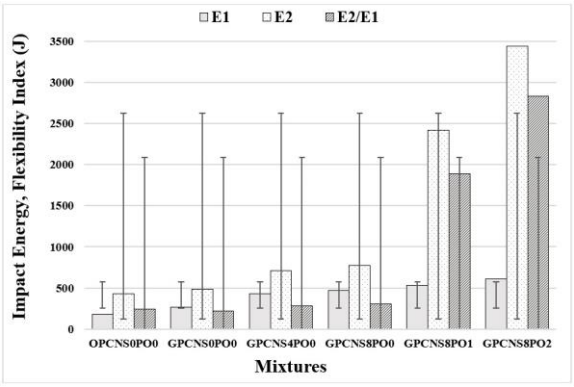

Fig. 5. The Impact Energy and The Flexibility Index of The Specimens

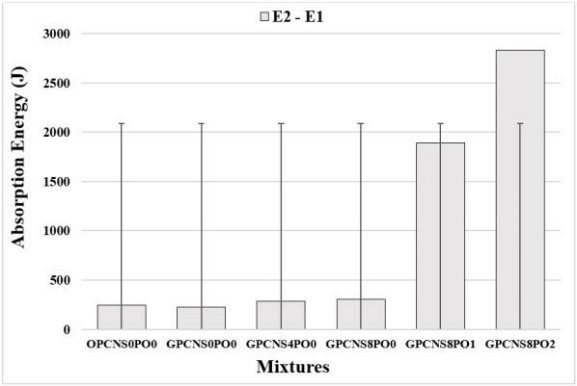

Fig. 6. Absorbed Energy of The Specimens

Table 6
Results of The Impact Resistance Tests

Mix ID	N_1	N_2	N_2-N_1	E_1(J)	E_2(J)	E_2-E_1 (J)	E_2/E_1 (J)
OPCNS0PO0	9	21	12	183	427	244	2.33
GPCNS0PO0	13	24	11	264	488	223	1.58
GPCNS4PO0	21	35	14	427	712	284	1.67
GPCNS8PO0	23	38	15	268	773	305	1.65
GPCNS8PO1	26	119	93	529	2422	1892	4.58
GPCNS8PO2	30	169	139	610	3439	2829	5.63

4. Results of the XRD, XRF and SEM Tests

The results obtained from the electron microscope can greatly help in identifying the structure and behavior of concrete. The mechanical and physical properties of the concrete matrix are considerably dependent on its microstructure. This section discusses the effect of NS and POFs on the microstructure of concrete paste using the SEM analysis.

Figure 7 shows the SEM of GPC containing NS reinforced with POFs (GPCNS8PO2). The role of briding in cracks and keeping concrete integrated by adding fibers can be seen in SEM image ((b) GPCNS8PO2), which has a great effect on increasing tensile strength and impact resistance. Although the fibers change the direction of the cracks or prevent many cracks, but its lack of chemical composition with the materials in GPC has reduced the strength and previous research on concrete shows a decrease in compressive strength of concretes containing poly olefin fiber. The addition of NS reduces this reduction and creates better adhesion between the fibers and the concrete paste [5].

Figure 8 shows the difference between SEM Portland cement and GBFS geopolymer. Research by others has shown that in Portland cement, C-S-H gels contain silicon groups organized in finite linear chains of the "dreierketten" structure, so they are mainly SiO_1 and SiO_2 species. Geopolymer is characterized by high polymerization materials with aluminosilicate structure, which is mainly composed of three cross-linked unit dimensions, including (SiO_4 (2Al) and SiO_4 (3A) [37]. Figure 9 shows the SEM of GBFS-based GPC containing NS. Obviously, NS-containing geopolymers show higher density and less porosity. This improvement can be attributed to two reasons. First, the nanoparticles fill the pores of the matrices, which reduces the porosity of the geopolymer nanocomposites, resulting in uniformity, less pores, and a more compact geopolymer matrix [5]. Second, the active silica particles improve the geopolymer reaction. In fact, the pozzolanic reaction condenses and homogenizes the microstructures by converting C-H to C-S-H [37], thus creating more geopolymer gel and a denser matrix [37] However, further increase in NS content causes insufficient dispersion and accumulation of NS particles, which slightly reduces matrix density [39].

The key difference between NS-containing and non-silica microstructures is that NS-containing microstructures are denser with fewer unreacted particles, resulting in a softer, more integrated structure. In the sample containing NS, very few fine cracks are observed, in which NS acts as a filler to fill the spaces inside the hardened microstructure skeleton of the geopolymer paste and increase its compaction [6, 40]. NS geopolymer matrices appear to be composed of a larger amount of amorphous crystalline compound.

Fig. 10 demonstrates the XRD results with a radiation intensity of Ka λ=1.54060 A-Cu. In order to perform this test, the central parts of the specimens were turned into a uniform homogeneous powder. The XRD analysis showed that most peaks in the GPC occurred in zones 15 to 35. However, for the ordinary

concrete, the zones of the peaks were larger, being from 15 to 50. Moreover, 60 peaks were observed due to the arrangement and atomic structure of the specimens. Therefore, by evaluating the formation angles of the peaks and their relative intensities, the types of the materials and peak phases of the XRD could be identified. In the ordinary concrete, aluminum phosphate ($AlPO_4$), calcium carbonate (CaC_6O_{18}), and calcium manganese carbonate ($Ca_7Mg_5C_{12}O_{36}$) had the highest dispersion, respectively. The largest peaks in the range of 25, 27, 29 and 60 angles are 3000, 22000, 2200 and 3000 cm^{-1}. In the GPC without NS, sodium aluminum silicate ($NaAlSi_3O_8$) and quartz (SiO_2) were dispersed due to the presence of GBFS and pozzolanic reactions. In the specimen containing 8% NS, $BiPO_4OOH$ and $Mg_{16}Si_{16}O_{48}$ were dispersed, and the percentage of the total silica increased. The range of peaks in geopolymer is between 27, 28 and 29.5 and the value of the largest peak for non-nano GPC is 1400, 850 and 2000 cm^{-1} and for sample 8% NS 1900, 4500 and 2100 cm^{-1}. The addition of NS increased the geopolymerization reaction. Therefore, a greater amount of amorphous geopolymer gel was created in the matrixes. In turn, this showed that the nanoparticles prevented the reduction in the geopolymer strength [5]. In general, the addition of amorphous NS to geopolymer pastes has resulted in minor changes in crystallinity and amorphous. With the addition of NS, the amorphous content mainly increases, which reduces the crystalline phase content. Because NS is amorphous, the increase in amorphous material in nanocomposite samples is usually attributed to the additional NS loaded in the pastes at the nan fill capacity [38, 41]. Strong peaks at 2200 and 1800 cm-1 are an Al-O-Si overlap and are interpreted asymmetric Si-O-Si tensile vibrations. It is widely known as the definitive peak and fingerprint of geopolymers (GBFS-based) [42] and the 4500 peak is due to the addition of NS, which is positioned 29 degrees. In XRD analysis, crystalline quartz is easily detected in the range 2θ=26-32. Which may be due to the formation of crystalline composition in the geopolymer matrix and it can be concluded that the strength of the sample (with NS) is higher than (without NS) due to the presence of more crystalline composition in the geopolymer matrix. The intensity of quartz, molite and hematite is higher due to the presence of additional materials in the sample matrix containing NS. Some additional peaks in NS-modified GPC indicate the formation of new phases of quartz (SiO_2), calcium carbonate, aluminum phosphate, compared to other samples, which confirms the presence of a crystalline phase in the geopolymer concrete. The chemical analysis of the GBFS-based GPC according to standard ASTM C989 [43] are provided in the following table.7 As shown in the XRF results in Table 6, By comparing GPC with ordinary concrete, In GPC the amount of SiO_2 and CaO reduced by 38%, while the amount of Na_2O and MgO significantly increased. With the addition of 8% NS, the amount of SiO_2 grew by 85%.

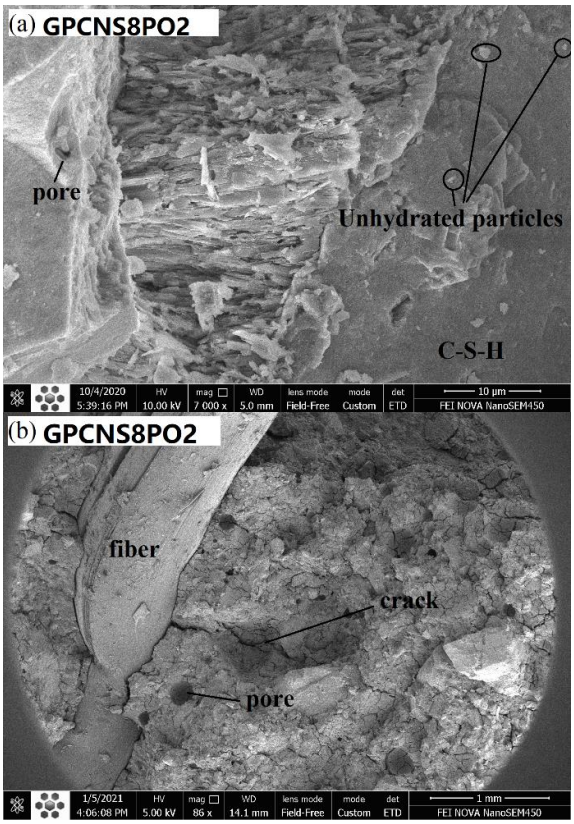

Fig. 7. Microstructure Image (SEM) of Geopolymer Concrete Reinforced with Polyolefin Fibers

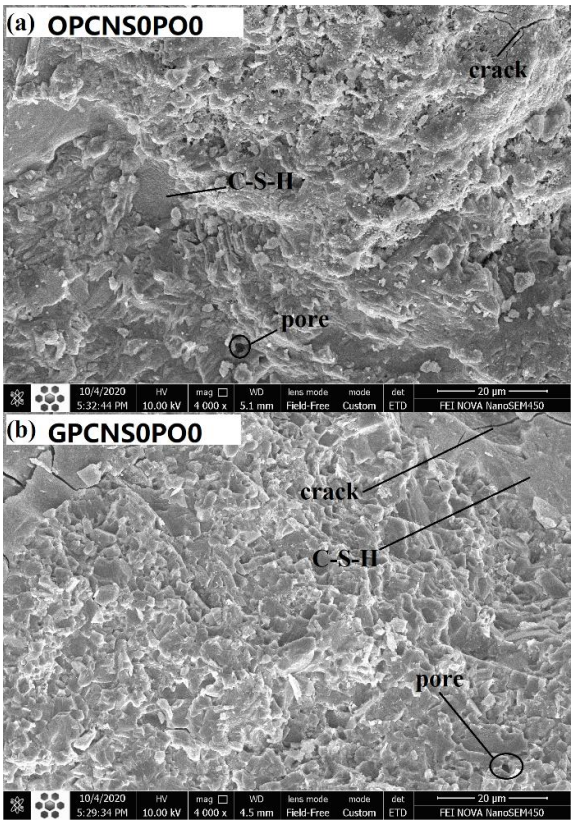

Fig. 8. Microstructure Image (SEM) of Geopolymer Concrete and Portland Cement Concrete

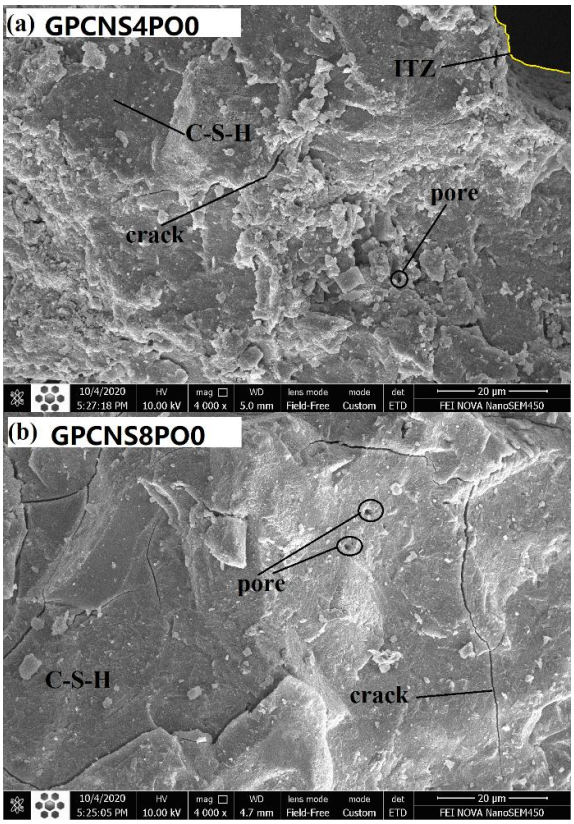

Fig. 9. Microstructure Image (SEM) of Geopolymer Concrete Containing NS

Table 7
XRF Test Values for Samples

Mix ID	SiO_2	AL_2O_3	CaO	MgO	K_2O	Na_2O	Fe_2O_3	LOI	TiO_2	SO_3
OPCNS0PO0	27.12	5.63	37.16	2.11	0.91	1.1	7.2	16.4	0.47	1.59
GPCNS0PO0	19.57	8.07	26.81	5.05	1.01	15.1	5.64	16.04	0.961	1.16
GPCNS4PO0	32.03	6.72	23.61	4.01	1.02	9.02	3.94	15.9	1.09	1.87
GPCNS8PO0	36.33	7.01	15.2	3.01	1.05	12.87	3.94	15.7	1.17	2.8

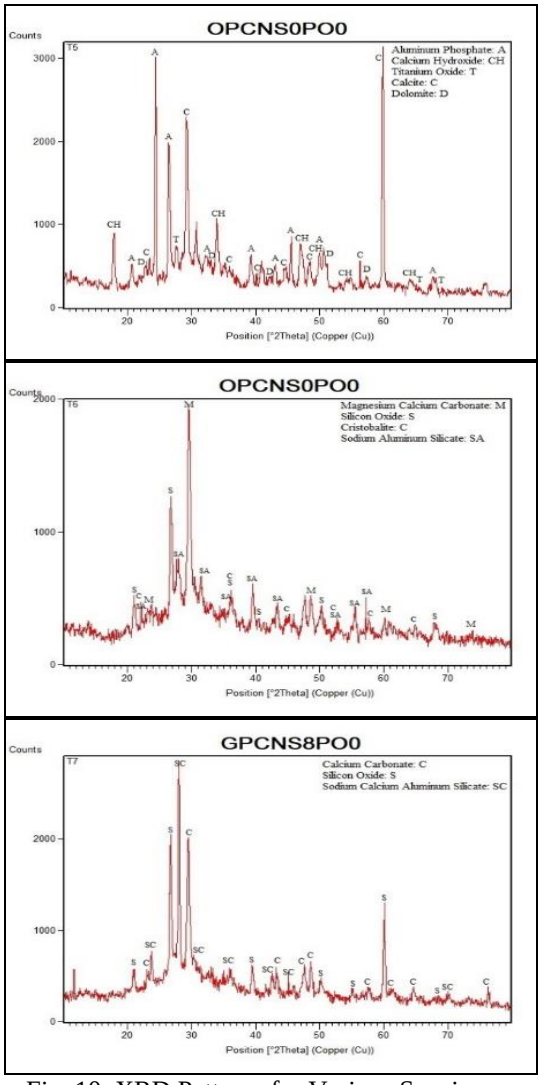

Fig. 10. XRD Patterns for Various Specimens

5. Conclusions

This study has evaluated the mechanical and microstructural properties of GBFS-based GPC containing POFs (0 to 2%) and NS (0 to 8%). The obtained results revealed that the addition of NS improved the mechanical and microstructural properties of the concrete. Furthermore, adding POFs remarkably affected the tensile strength and impact resistance.

1. The addition of NS to the GBFS-based GPC increased the compressive strength by 20% from 68 MPa to 82 MPa. The addition of fibers reduced the compressive strength of the specimens.
2. The fibers also improved the tensile strength due to the role of fibers in connection the cracks, brittle rupture and crushing of the specimen are prevented. It was found that the addition of NS increased the tensile strength by 11% to 15%.
3. The elastic modulus tests revealed that the elastic modulus increased by adding fibers and NS and replacing the ordinary concrete with GPC.
4. The impact resistance results indicated the marked effect of POFs on the number of impacts required for the creation of the first crack and full failure, increasing them by 13-30% and 213-345%, respectively. It was also found that the addition of NS increased the absorbed energy by 62% to 77%.
5. The results of the UPV tests indicated the excellent quality of all specimens at the ages of 28 and 90 days. Filling the pores and integrating the concrete, NS increased the velocity of the passing pulses.
6. The results of SEM, XRD and XRF tests were in coordination with the results of all tests performed in this study and well demonstrated the filling of the pores by the nanoparticles and densification of the concrete.

References

[1] Siddique, R. and D. Kaur, *Properties of concrete containing ground granulated blast furnace slag (GGBFS) at elevated temperatures.* Journal of Advanced Research, 2012. 3(1): p. 45-51.

[2] Yüksel, İ., R. Siddique, and Ö. Özkan, *Influence of high temperature on the properties of concretes made with industrial by-products as fine aggregate replacement.* Construction and building materials, 2011. 25(2): p. 967-972.

[3] McNulty, E., *Geopolymers: an environmental alternative to carbon dioxide producing ordinary Portland cement.* Department of Chemistry, The Catholic University of America, 2009.

[4] Aslani, F., *Thermal performance modeling of geopolymer concrete.* Journal of Materials in Civil Engineering, 2016. 28(1): p. 04015062.

[5] Assaedi, H., et al., *Influence of nano silica particles on durability of flax fabric reinforced geopolymer composites.* Materials, 2019. 12(9): p. 1459.

[6] Deb, P.S., P.K. Sarker, and S. Barbhuiya, *Effects of nano-silica on the strength development of geopolymer cured at room temperature.* Construction and building materials, 2015. 101: p. 675-683.

[7] Adak, D., M. Sarkar, and S. Mandal, *Structural performance of nano-silica modified fly-ash based geopolymer concrete.* Construction and Building Materials, 2017. 135: p. 430-439.

[8] Ekinci, E., et al., *The improvement of mechanical, physical and durability characteristics of volcanic tuff based geopolymer concrete by using nano silica, micro silica and Styrene-Butadiene Latex additives at different ratios.* Construction and Building Materials, 2019. 201: p. 257-267.

[9] Yousefvand, M., Y. Sharifi, and S. Yousefvand, *An Analysis of the Shear Strength and Rupture Modulus of Polyolefin-Fiber Reinforced Concrete at Different Temperatures.* Journal of civil Engineering and Materials Application, 2019. 3(4): p. 238-254.

[10] Rashad, A.M., *The effect of polypropylene, polyvinyl-alcohol, carbon and glass fibres on geopolymers properties.* Materials Science and Technology, 2019. 35(2): p. 127-146.

[11] Chellapandian, M., A. Mani, and S.S. Prakash, *Effect of macro-synthetic structural fibers on the flexural behavior of concrete beams reinforced with different ratios of GFRP bars.* Composite Structures, 2020. 254: p. 112790.

[12] Adhikary, S.K., et al., *Investigation on the mechanical properties and post-cracking behavior of polyolefin fiber reinforced concrete.* Fibers, 2019. 7(1): p. 8.

[13] Noushini, A., A. Castel, and R.I. Gilbert, *Creep and shrinkage of synthetic fibre-reinforced geopolymer concrete.* Magazine of Concrete Research, 2019. 71(20): p. 1070-1082.

[14] Noushini, A., et al., *Mechanical and flexural performance of synthetic fibre reinforced geopolymer concrete.* Construction and Building Materials, 2018. 186: p. 454-475.

[15] Pilehvar, S., et al., *Physical and mechanical properties of fly ash and slag geopolymer concrete containing different types of micro-encapsulated phase change materials.* Construction and Building Materials, 2018. 173: p. 28-39.

[16] EN, B., *Testing hardened concrete. Method of determination of compressive strength of concrete cubes.* BS EN 12390 Part, 2000. 3.

[17] ASTM, C.-. *Standard Test Method for Splitting Tensile Strength of Cylindrical Concrete Specimens.*

[18] ASTM C469 / C469M-14, Standard Test Method for Static Modulus of Elasticity and Poisson's Ratio of Concrete in Compression, ASTM International, West Conshohocken, PA, 2014.

[19] Galan, A. *Estimate of concrete strength by ultrasonic pulse velocity and damping constant*. in *Journal Proceedings*. 1967.

[20] 544-2R-89, A., *'Measurement of properties of fiber reinforced concrete'.* Reported by ACI Committee, 1999. 544.

[21] Wang, K., S.P. Shah, and P. Phuaksuk, *Plastic shrinkage cracking in concrete materials-Influence of fly ash and fibers.* ACI Materials Journal, 2002. 99(5): p. 512-513.

[22] Beigi, M.H., et al., *An experimental survey on combined effects of fibers and nanosilica on the mechanical, rheological, and durability properties of self-compacting concrete.* Materials & Design, 2013. 50: p. 1019-1029.

[23] Deb, P.S., P.K. Sarker, and S. Barbhuiya, *Sorptivity and acid resistance of ambient-cured geopolymer mortars containing nano-silica.* Cement and Concrete Composites, 2016. 72: p. 235-245.

[24] Law, D.W., et al., *Long term durability properties of class F fly ash geopolymer concrete.* Materials and Structures, 2015. 48(3): p. 721-731.

[25] Bahadori, H. and P. Hosseini, *Reduction of cement consumption by the aid of silica nano-*

particles (investigation on concrete properties). Journal of Civil Engineering and Management, 2012. 18(3): p. 416-425.

[26] Bosiljkov, V.B., *SCC mixes with poorly graded aggregate and high volume of limestone filler.* Cement and Concrete Research, 2003. 33(9): p. 1279-1286.

[27] 363, A.C. *State-of-the-art Report on High-strength Concrete (ACI 363R-84)*. 1984. American Concrete Institute.

[28] Nath, P. and P.K. Sarker, *Flexural strength and elastic modulus of ambient-cured blended low-calcium fly ash geopolymer concrete.* Construction and Building Materials, 2017. 130: p. 22-31.

[29] Diaz-Loya, E.I., E.N. Allouche, and S. Vaidya, *Mechanical properties of fly-ash-based geopolymer concrete.* ACI materials journal, 2011. 108(3): p. 300.

[30] 363, A.C., *State of the art of high strength concrete.* American Concrete Institute, (1993).

[31] Sumajouw, D., et al., *Fly ash-based geopolymer concrete: study of slender reinforced columns.* Journal of materials science, 2007. 42(9): p. 3124-3130.

[32] IS 13311-1): Method of Non-destructive testing ofconcret, Part 1: Ultrasonic pulse velocity [CED 2: Cement and Concrete], Delhi, India, 1992.

[33] Sahmaran, M., A. Yurtseven, and I.O. Yaman, *Workability of hybrid fiber reinforced self-compacting concrete.* Building and Environment, 2005. 40(12): p. 1672-1677.

[34] Whitehurst, E.A. *Soniscope tests concrete structures*. in *Journal Proceedings*. 1951.

[35] Kwan, W.H., et al., *Influence of the amount of recycled coarse aggregate in concrete design and durability properties.* Construction and Building Materials, 2012. 26(1): p. 565-573.

[36] Ren, W., J. Xu, and E. Bai, *Strength and ultrasonic characteristics of alkali-activated fly ash-slag geopolymer concrete after exposure to elevated temperatures.* Journal of Materials in Civil Engineering, 2015. 28(2): p. 04015124.

[37] Du, H., S. Du, and X. Liu, *Durability performances of concrete with nano-silica.* Construction and building materials, 2014. 73: p. 705-712.

[38] Phoo-ngernkham, T., et al., *The effect of adding nano-SiO2 and nano-Al2O3 on properties of high calcium fly ash geopolymer cured at ambient temperature.* Materials & Design, 2014. 55: p. 58-65.

[39] Supit, S.W.M. and F.U.A. Shaikh, *Durability properties of high volume fly ash concrete containing nano-silica.* Materials and structures, 2015. 48(8): p. 2431-2445.

[40] Shih, J.-Y., T.-P. Chang, and T.-C. Hsiao, *Effect of nanosilica on characterization of Portland cement composite.* Materials Science and Engineering: A, 2006. 424(1-2): p. 266-274.

[41] Nazari, A. and J.G. Sanjayan, *Hybrid effects of alumina and silica nanoparticles on water absorption of geopolymers: Application of Taguchi approach.* Measurement, 2015. 60: p. 240-246.

[42] Phair, J. and J. Van Deventer, *Effect of the silicate activator pH on the microstructural characteristics of waste-based geopolymers.* International Journal of Mineral Processing, 2002. 66(1-4): p. 121-143.

[43] C989/C989M-18a, A., *Standard specification for slag cement for use in concrete and mortars*. 2018, ASTM International West Conshohocken, PA.